Magnetocaloric effect in the vicinity of the magnetic phase transition in NdCo$_{2-x}$Fe$_x$ compounds

Adil Murtaza,[1] Wenliang Zuo,[1] Muhammad Yaseen ⓘ,[2] Awais Ghani,[1] Azhar Saeed ⓘ,[1] Chunxi Hao,[1] Jingwen Mi,[1] Yebei Li,[1] Tieyan Chang ⓘ,[1] Liqun Wang,[1] Chao Zhou ⓘ,[1] Yu Wang,[1] Yin Zhang,[1] Sen Yang ⓘ,[1,*] and Yang Ren[3]

[1]*MOE Key Laboratory for Nonequilibrium Synthesis and Modulation of Condensed Matter, State Key Laboratory for Mechanical Behavior of Materials, Xi'an Jiaotong University, Xi'an 710049, China*
[2]*Department of Physics, University of Agriculture, Faisalabad, 38040, Pakistan*
[3]*X-Ray Science Division, Argonne National Laboratory, Argonne, Illinions 60439, USA*

In the present paper, the magnetocaloric effect (MCE) of NdCo$_{2-x}$Fe$_x$ ($x = 0$, 0.2, 0.4, 0.6) compounds was investigated by magnetization measurements. The temperature-dependent high-resolution synchrotron x-ray diffraction study shows a magnetostructural transition from the paramagnetic cubic phase to the ferromagnetic tetragonal phase below their Curie temperatures. Differential scanning calorimetry analysis shows the absence of thermal hysteresis, indicating the second-order nature of the magnetostructural phase transition in these compounds. The maximum values of magnetic entropy change (ΔS_M) and wide operating temperature (OT) are obtained under a field change of 5 T, which are 7.33 Jkg^{-1}K^{-1}, 6.45 Jkg^{-1}K^{-1}, 5.71 Jkg^{-1}K^{-1}, 4.70 Jkg^{-1}K^{-1} and 78 K, 82 K, 85 K, 92 K for $x = 0$, 0.2, 0.4, and 0.6, respectively. The corresponding values of relative cooling power (RCP) are 529.96 Jkg^{-1}, 497.25 Jkg^{-1}, 470.55 Jkg^{-1}, and 428.31 Jkg^{-1}. The observed wide OT range and large RCP values are comparable with Gd, Gd$_5$Ge$_2$Si$_2$, and some rare-earth-based giant magnetocaloric materials, making this series of compounds suitable for magnetic refrigeration.

I. INTRODUCTION

In the few past years, magnetic materials with both magnetic and structural phase transitions have attracted considerable attention because of their unique and novel physical properties and possible vast applications in advanced technologies [1–4]. Among those, the rare-earth (R)-based Laves phase compounds are quite interesting in condensed-matter physics, materials science, and engineering due to their simple magnetic and crystallographic structures to validate different physical models [5–7]. They are considered as suitable materials to study different properties such as magnetoelasticity, magnetocaloric effect (MCE), and magnetoelectric (ME) phenomena because of high magnetostriction (λ_S), large magnetic entropy change (ΔS_M), and magnetoresistance (ΔM_R), respectively [3,4]. Among various properties of, the MCE being a magnetothermodynamic phenomenon is another important feature that can be used for magnetic refrigeration technology due to its high thermodynamic efficiency, ecological concerns, and a large probability of applications in a wide temperature span as compared to the conventional vapor compression refrigerators [8–11]. For this purpose, MCE has been studied widely in different types of materials, e.g., R-containing and R-free crystalline materials [12,13], Gd-based compounds including Gd$_5$Si$_2$Ge$_2$ [14], Heusler alloys [15], MnAs-based alloys [16], multiphase materials and composites [17,18], and nanostructured materials [19]. Although MCE is an intrinsic property of all magnetic materials, especially RCo$_2$-based compounds are expected to show large ΔS_M,

because the observed large R magnetic moment values are close to their free ion values [20]. The RCo$_2$ compounds with the first-order magnetic transition (FOMT) e.g., DyCo$_2$ [21], HoCo$_2$ [22], ErCo$_2$ [23] are the most promising candidates for MCE, owing to their large ΔS_M around their phase transition temperature (T_C). But at the same time, these materials exhibit remarkable thermal and magnetic hysteresis and possess narrow working temperature range, which causes an obvious decrease in the relative cooling power (RCP); a quality factor to determine the efficiency of MCE [24]. To overcome these problems, the materials undergoing a second-order magnetic transition (SOMT), for example, TbCo$_2$, TmCo$_2$, and PrCo$_2$ can be used as alternative materials [4,25]. These materials generally show smaller ΔS_M than giant MCE materials, however, they possess narrow thermal hysteresis. Besides, their ΔS_M can be extended through a wide temperature range, which increases the effective RCP values [26]. Because of the lack of thermal hysteresis and the possibility of high RCP, materials with SOMT can be used as an alternative for designing magnetic refrigerator prototypes. Despite the intensive research on magnetic and magnetocaloric properties of R-based compounds, there are very rare studies on MCE in NdCo$_2$ compounds. Hence, it is worthy to study the MCE in NdCo$_2$ compounds. Among the RCo$_2$ (R = Tb, Dy, Er, Ho, Gd, Tm, Pr, and Sm) series, NdCo$_2$ shows the paramagnetic (PM) to ferromagnetic (FM) transition (second order) along with a structural transition from cubic (space group $Fd\bar{3}m$) to a tetragonal (space group $I4_1/amd$) when cooled below $T_C \approx 100$ K. With the further decrease in temperature, a structural transition from tetragonal to orthorhombic (space group $Imma$) along with spin reorientation (T_{SR}) (which is FOMT) is observed at 42 K [27,28]. Due to this simultaneous occurrence

*yang.sen@mail.xjtu.edu.cn

of structural and magnetic transitions, a large MCE can be expected in this compound. Moreover, its low T_C can be tuned even up to room temperature (RT) by changing the ratio of constituent elements or by substituting a sufficient amount of $3d$ elements (Fe) for Co as shown by other researchers [29,30]. Recently Zheng *et. al* reported the MCE in $Nd(Co_{0.8}Fe_{0.2})_2$ Laves compound, where a large refrigerant capacity with negligible thermal and magnetic hysteresis was observed in the PM-FM transition region [31]. In the present study, we investigated the magnetic and magnetocaloric properties in a series of $NdCo_{2-x}Fe_x$ ($x = 0$, 0.2, 0.4, 0.6) compounds to explore several important aspects of these compounds, which were not considered previously. First, through *in situ* synchrotron XRD measurements, we explored the effect of Fe substitution on the structural transition and its corresponding relation with the MCE. As discussed earlier, the FOMT usually leads to considerable thermal and magnetic hysteresis that will consume the RCP of magnetic refrigerant materials. Therefore, we focused our studies around the SOMT. The results indicate that these compounds exhibit a wide working temperature range around the phase transition and deliver large RCP with negligible thermal hysteresis. Second, we have shown that substitution of Fe up to different levels not only tunes the phase transition temperature but also broadens the working temperature range without any change in SOMT character. For example, the working temperature range of under studies compounds is wider than that of Gd [32] and $Gd_5Si_2Ge_2$ [33] at the field changes of 2 T and 5 T. Their magnetocaloric performance is comparable or even better than some earlier reported *R*-based giant magnetic refrigerant materials. What's more, Nd is much cheaper than those heavy *R* elements (Tb, Dy, Ho, etc). These prominent features reveal the applicability of $NdCo_{2-x}Fe_x$ materials in ecologically friendly magnetic refrigeration. A detailed structural and magnetic characterization of these compounds shed light on the magnetic and magnetocaloric properties in RCo_2 compounds, which is helpful to understand technological exploitation of such kinds of materials.

II. EXPERIMENTAL PROCEDURES

A series of $NdCo_{2-x}Fe_x$ ($0 \leqslant x \leqslant 1.0$) compounds with nominal compositions were prepared by melting the high-purity Nd (99.9% pure) and Fe/Co(99.9% pure) in an arc furnace under a purified argon atmosphere. To obtain better chemical homogeneity, the ingots were melted five times. Subsequently, the melted samples were sealed in evacuated quartz tubes, annealed at 973 K for seven days, and then naturally cooled in the furnace to room temperature. The phase and crystal structures were determined by high-resolution synchrotron XRD with beamline 11-IDC, at Advanced Photon Source, Argonne National Laboratory, USA. For this purpose, a small amount of the samples (0.5 g) were ground into powders and sealed in quartz capillaries with a diameter of 0.3 mm. The wavelength of the synchrotron x ray was 0.11725 Å. During the synchrotron XRD measurement, the capillary was rotated to average the intensity and to reduce the preferred orientation effect. Diffraction patterns were analyzed by the Rietveld refinement method using FULL-PROF software [34]. Differential scanning calorimetry (DSC)

measurements were carried out using TA Instruments Q2000 during heating and cooling cycles with a scanning rate of 5 K/min. Magnetic characterizations were performed by using SQUID (Quantum Design). The magnetic susceptibility (χ_{AC}) was measured in an AC-driving field of amplitude of 500 Oe and a frequency of 300 Hz. The Curie temperatures were determined by magnetization (M) versus temperature (T) curves measured in field-cooled (FC) and zero-field cooled (ZFC) modes under applied field of 500 Oe. In ZFC, the sample was first cooled down from 400 K (PM state) to 90 K in the absence of applied magnetic field. Later, magnetization (M_{ZFC}) was recorded during the warming of the sample from 90 K to 400 K in the presence of applied magnetic field whereas for FC magnetization, the sample was cooled down in the presence of an applied magnetic field and temperature dependence magnetization (M_{FC}) was measured during the warming cycle from 90 K to 400 K. The isothermal magnetization $M(H)$ curves were measured under the field of 6 T at different temperatures below and above T_C under field decreasing and increasing modes. Before starting the measurement, initially, the sample was cooled down to the desired temperature in zero applied field, and the $M(H)$ curves were measured by increasing magnetic field from 0 T to a predetermined maximum 6 T and then decreasing magnetic field from 6 T back to 0 T. After one isothermal curve was measured, the temperature was increased slowly with step scan of 3 K to measure another curve under increasing and decreasing field processes. The ΔS_M was evaluated from M-H curves by using Maxwell's equation.

III. RESULTS AND DISCUSSION

A. Crystal structural analysis by *in situ* high-resolution XRD

Phase identification and structural analysis of $NdCo_{2-x}Fe_x$ compounds was carried out by high-resolution synchrotron x-ray diffraction at different temperatures. The detailed structural investigations of all the samples were carried out by refining the XRD data using the Rietveld method [1]. In this refinement, the experimental data (Y_{EXP}) are represented by black stars, the calculated patterns (Y_{CAL}) are represented by solid red lines, and the difference between Y_{EXP} and Y_{CAL} is shown by the bottom curve (blue line). The Bragg positions are shown in the vertical marks just under the profile. The refined diffraction patterns for $NdCo_2$ and $NdCo_{1.6}Fe_{0.4}$ samples are shown in Fig. 1. The remaining two samples ($NdCo_{1.8}Fe_{0.2}$) and ($NdCo_{1.4}Fe_{0.6}$) are shown in the Supplemental Material, Fig. 1. [35]. Refinement analysis shows that all the samples predominantly consist of 1:2-type phase. However, some additional peaks corresponding to the secondary 1:3 type minor phase with $PuNi_3$ Laves phase structure was also observed; it does not show an obvious change at different temperatures. The main diffraction peaks of a major phase (1:2 type) are indexed as related to the $MgCu_2$-type cubic Laves phase structure. The fractions of observed phases were determined through refinement for all the studied samples and are tabulated in Table I. It is clear that the 1:2 type major phase (>95 %) dominates over the secondary phase in all four samples. The appearance of a 1:3-like secondary phase might be due to the high annealing temperature of 973 K,
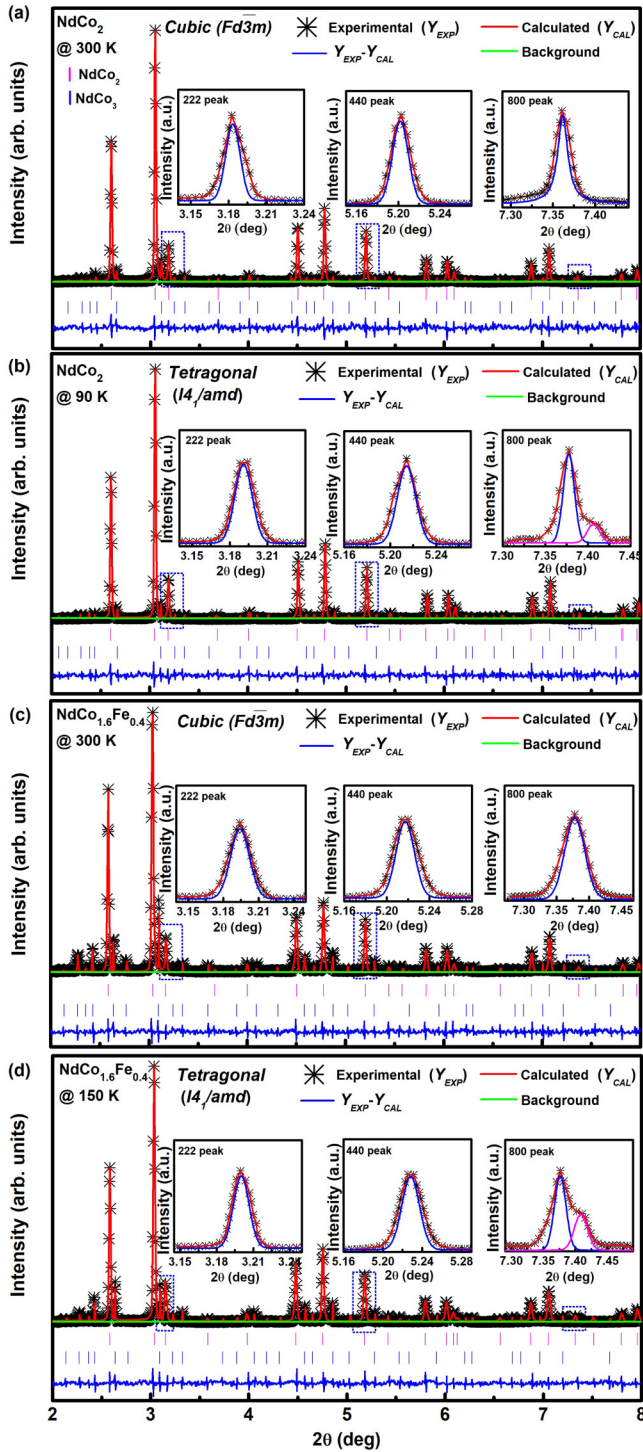
FIG. 1. Structural analysis of the $NdCo_{2-x}Fe_x$ system. Synchrotron x-ray diffraction data with Rietveld refinement for (a) $NdCo_2$ at 300 K and 90 K (b). $NdCo_{1.6}Fe_{0.4}$ at 300 K and 150 K. Black stars correspond to experimental data (Y_{EXP}), and the red lines are calculated patterns (Y_{CAL}). The green line is the background used in the refinement. The vertical bars just below the plots represent the calculated positions of Bragg reflections correspond to crystal structures. The difference between the experimental data and calculated patterns is shown by blue color solid lines at the bottom of each pattern. The insets show the enlarged main characteristic reflections of (222), (440), and (800) peaks.

which partially converts the 1:2 type phase into a 1:3 type phase, as reported in other Laves compounds [36]. This also indicates the importance of suitable annealing temperature to prepare 1:2 type single-phase compounds, and thus requires further research to formulate the suitable heat treatment process to prepare a homogeneous alloy and avoid the non-$MgCu_2$-type phase simultaneously. Refinement results reveal that the $NdCo_2$ and $NdCo_{1.6}Fe_{0.4}$ samples at room temperature (RT = 300 K) crystallizing in the cubic structure. For clarity, the enlarged main characteristic reflections of (222), (440), and (800) peaks are presented in the insets of Figs. 1(a) and 1(c). It can be clearly seen that the characteristic reflections of (222), (440), and (800) show no splitting and can be fitted by using a single peak. These features characterize a cubic structure with space group of $Fd\bar{3}m$ in which Nd atoms occupy the $8a$ (0.125, 0.125, 0.125) atomic sites, and Co/Fe atoms occupy the $16d$ sites (0.5, 0.5, 0.5) [37]. The calculated lattice parameters and unit cell volume are $a = 7.297$ Å, $V = 388.53$ Å, and $a = 7.317$ Å, $V = 391.74$ Å for $NdCo_2$ and $NdCo_{1.6}Fe_{0.4}$, respectively. However, with decreasing temperature from RT to 90 K for $x = 0$ ($NdCo_2$) and to 150 K for $x = 0.4$ ($NdCo_{1.6}Fe_{0.4}$), a structural transition occurs accompanied by the magnetic phase transition and the crystal structure changes from cubic phase to tetragonal phase. The characteristic (222) and (440) reflections can be fitted by using a single peak indicating no splitting in (222) and (440) reflections. However, the characteristic (800) reflections split into two peaks which can be fitted by using double peaks as shown in insets of Figs. 1(b) and 1(d). These features characterize a tetragonal structure having an easy magnetization direction (EMD) along the [100] axis. Its corresponding space group is $I4_1/amd$, in which Nd atoms occupy the $4b$ sites (0, 1/4, 3/8), and Co/Fe atoms occupy the $8c$ sites (0, 0, 0). The lattice parameters and unit cell volume were found to be $a = b = 7.287$ Å, $c = 7.255$ Å, $V = 385.24$ Å, and $a = b = 7.293$ Å, $c = 7.258$ Å, $V = 386.0$ Å for $NdCo_2$ and $NdCo_{1.6}Fe_{0.4}$, respectively. These results agree well with the neutron powder diffraction analysis for $NdCo_2$ [28]. The schematic diagrams of the crystallographic structures corresponding to cubic and tetragonal phases, which were created by using the VESTA code are displayed in Fig. 2. Although Fe substitution with $x = 0 - 0.6$ does not change the structure type, a slight shifting in the XRD peaks toward a small angle indicates the increase of the lattice parameters and unit cell volume in the Fe substituted samples compared with the parent compound $NdCo_2$, and this increasing behavior is due to the larger size of Fe atoms ($r_{Fe} = 1.4$ Å) compared to Co atoms ($r_{Co} = 1.35$ Å) [38]. Refined crystallographic data, the unit cell, and other fitting parameters are summarized in Table I. The significant values of Rf factor and Bragg R_B factors (referring to the crystallographic and the reflected intensities), profile reliability factors R_p (profile fitting R value), R_{wp} (weighted profile R value) and χ^2 (goodness-of-fit quality factor) indicate a good fitting between Y_{EXP} and Y_{CAL}.

B. Temperature-dependent magnetization (M-T)

To obtain thermomagnetic properties and magnetic transitions, the temperature dependence of FC and ZFC magnetization under a field of 500 Oe was measured for the

TABLE I. Experimental details, Phase identified and their fraction, and refined crystal structure parameters of $NdCo_2$, $NdCo_{1.8}Fe_{0.2}$, $NdCo_{1.6}Fe_{0.4}$ and $NdCo_{1.6}Fe_{0.4}$ samples at different temperatures.

Wavelength (λ)	0.11725(Å)			
$2(\theta)$ scan range	$2–8^o$			
Step size $2(\theta)$	0.001^o			
Program	FULLPROF			
Sample	$NdCo_2$	$NdCo_{1.8}Fe_{0.2}$	$NdCo_{1.6}Fe_{0.4}$	$NdCo_{1.4}Fe_{0.6}$
Temperature (K)	300	300	300	
	$(T > T_C)$	$(T > T_C)$	$(T > T_C)$	
Phase identified	Phase fraction (%)			
1:2 type-phase (major) ($MgCu_2$)	96.4	97.3	95.1	
1:3 type-phase (minor) ($PuNi_3$)	3.6	2.7	4.9	
Structure	Cubic			
Space group	$Fd\bar{3}m$			
Lattice parameters				
$a = b = c$ (Å)	7.297	7.305	7.317	
Volume (V)(Å)	388.53	389.81	391.74	
Atom site (Nd)	$8a$ (1/8, 1/8, 1/8)	$8a$ (1/8, 1/8, 1/8)	$8a$ (1/8, 1/8, 1/8)	
B(Å)^2	0.65	0.64	0.67	
Atom site (Co/Fe)	$16d$ (1/2, 1/2,1/2)	$16d$ (1/2, 1/2,1/2)	$16d$ (1/2, 1/2,1/2)	
B(Å)^2	0.63	0.58	0.61	
R_p(%)	4.32	4.61	5.29	
R_{WP}(%)	5.31	5.72	6.21	
χ^2	2.51	2.34	2.32	
R_B	4.15	3.95	4.34	
R_F	3.25	3.19	3.10	
Temperature (K)	90	150	150	250
	$(T < T_C)$	$(T < T_C)$	$(T < T_C)$	$(T < T_C)$
Recognized phases	Phase fraction (%)			
1:2-type phase (major) ($MgCu_2$)	96.8	97.7	95.4	97.3
1:3-type phase (minor) ($PuNi_3$)	3.2	2.3	4.6	2.7
Structure	Tetragonal			
Space group	$I41/amd$			
Lattice parameters				
a=b (Å)	7.287	7.29	7.293	7.309
c (Å)	7.255	7.257	7.258	7.261
Volume (V) (Å)	385.24	385.67	386.03	387.89
Atom site (Nd)	$4b$ (0, 1/4, 3/8)	$4b$ (0, 1/4, 3/8)	$4b$ (0, 1/4, 3/8)	$4b$ (0, 1/4, 3/8)
B(Å)^2	0.29	0.32	0.45	0.39
Atom site (Co/Fe)	$8c$ (0, 0, 0)	$8c$ (0, 0, 0)	$8c$ (0, 0, 0)	$8c$ (0, 0, 0)
B(Å)^2	0.35	0.39	0.51	0.42
R_p(%)	5.97	4.65	4.98	4.55
R_{WP}(%)	7.92	7.71	7.86	7.61
χ^2	2.43	2.51	2.57	2.48
R_B	3.19	3.24	3.36	3.29
R_F	2.79	2.63	2.57	2.67

$NdCo_{2-x}Fe_2$ ($x = 0$, 0.2, 0.4, and 0.6) as shown in Fig. 3. The studied compounds clearly exhibit a single transition from high-temperature PM to low-temperature FM behavior at corresponding T_C. The T_C was derived by the position of the first derivative (dM/dT) peaks on the temperature axis. For $x = 0$, 0.2, 0.4, and 0.6, a normal PM-FM transition occurs at 102 K, 117 K, 255 K, and 345 K, respectively.

It is interesting to note that by 30% substitution of Fe for Co, the T_C can be increased to 345 K. Obviously, this increase is attributed to the stronger exchange interactions in the $3d$-ion subsystems, which mainly determines the T_C of RCo_2 compounds. Under the applied field of 500 Oe, the FC magnetization curves of all studied compositions indicate the irreversible behavior before the maxima showing
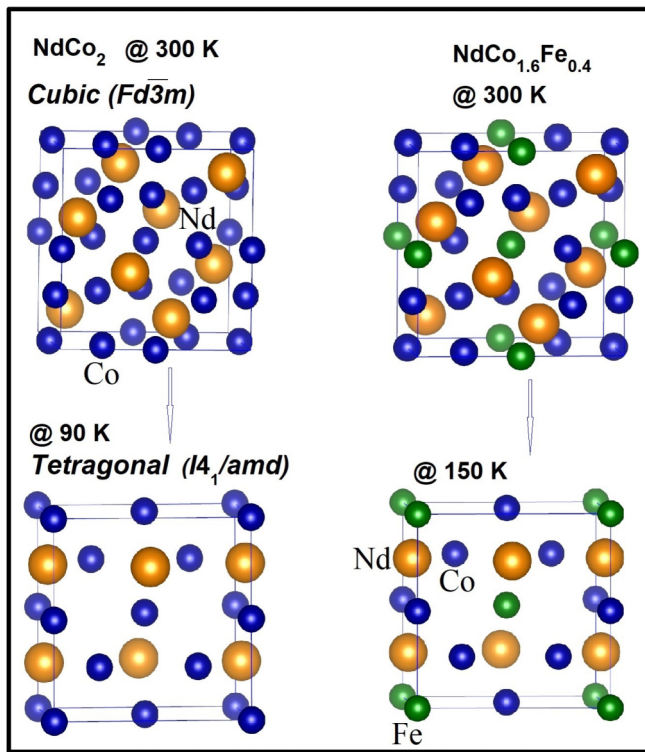
FIG. 2. The schematic diagrams of the crystal structure of the cubic phase ($Fd\bar{3}m$ space group) and tetragonal phase ($I4_1/amd$ space group) for $NdCo_2$ (on the left) and $NdCo_{1.6}Fe_{0.4}$ (on the right). The blue, green, and yellow balls represent Co, Fe, and Nd atoms, respectively.

large magnetization than ZFC, which signals the SOMT. Both the FC and ZFC curves are overlapped with each other around and above T_C, which indicates no thermal hysteresis in these compounds; making them potentially interesting for MCE application. However, at low temperatures a clear bifurcation between FC and ZFC curves is observed. This difference is also known as the thermomagnetic irreversibility and has observed in many compounds [39,40], revealing that such a behavior arises due to the domain wall pinning or may be related to the complex nature of magnetic transition at T_C, or due to the noncollinearity of magnetic structure below T_C due to crystal field effect in highly anisotropic magnetic materials [41].

In the PM state (above T_C), the inverse magnetic susceptibility (T-χ^{-1}) follows nicely the Curie-Weiss law $\chi^{-1} = (T + \theta_P)/C$ [42], as shown in the right-hand side axis of Fig. 3. Here, θ_P is the PM Curie temperature and C is the Curie constant, which is related to the effective magnetic moment (μ_{eff}) of Tb ions in the PM state. From the linear fit of inverse magnetic susceptibility, the evaluated values of θ_P and μ_{eff} are 103 K, 119 K, 256 K, 346 K, and 3.31 μ_B, 3.26 μ_B, 3.20 μ_B, 2.99 μ_B for $x = 0$, 0.2, 0.4, and 0.6, respectively. The positive θ_P suggests that the FM interactions are dominant in these compounds. Besides, the values of θ_P are a little higher than T_C, the origin of this difference is related to the presence of a short-ordered range slightly greater than T_C.

Recent studies reveal that the FM transition is always coupled to the lattice and causes a simultaneous structural change,
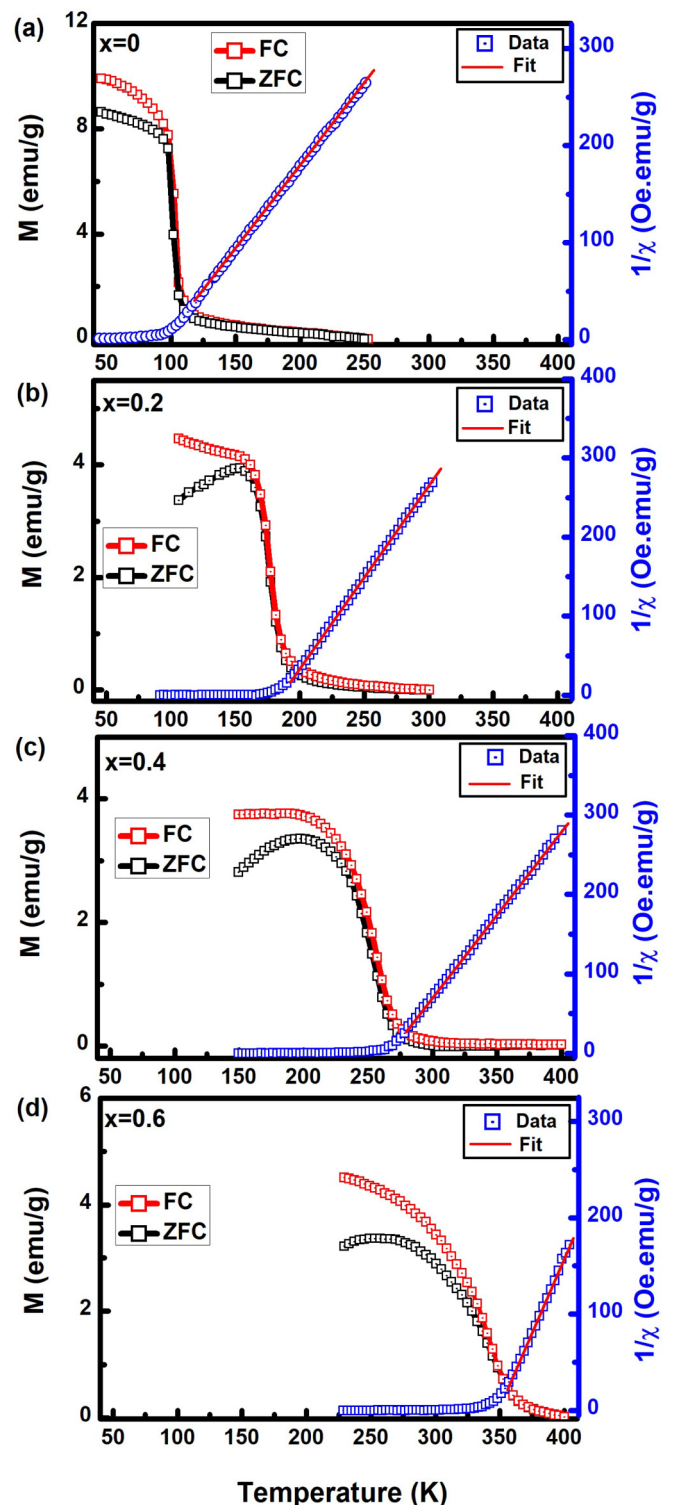
FIG. 3. Temperature dependence of ZFC and FC magnetization curves under 500 Oe magnetic field (left-side scale) and inverse magnetic susceptibility (right-hand scale) for $NdCo_{2-x}Fe_x$ ($x = 0$, 0.2, 0.4, 0.6) compounds.

yielding a low crystallographic symmetry that conforms to the spontaneous magnetization (M_S) direction [43]. Our *in situ* XRD and *M-T* results clearly show that $NdCo_{2-x}Fe_x$ compounds undergo a magnetostructural transition from a PM
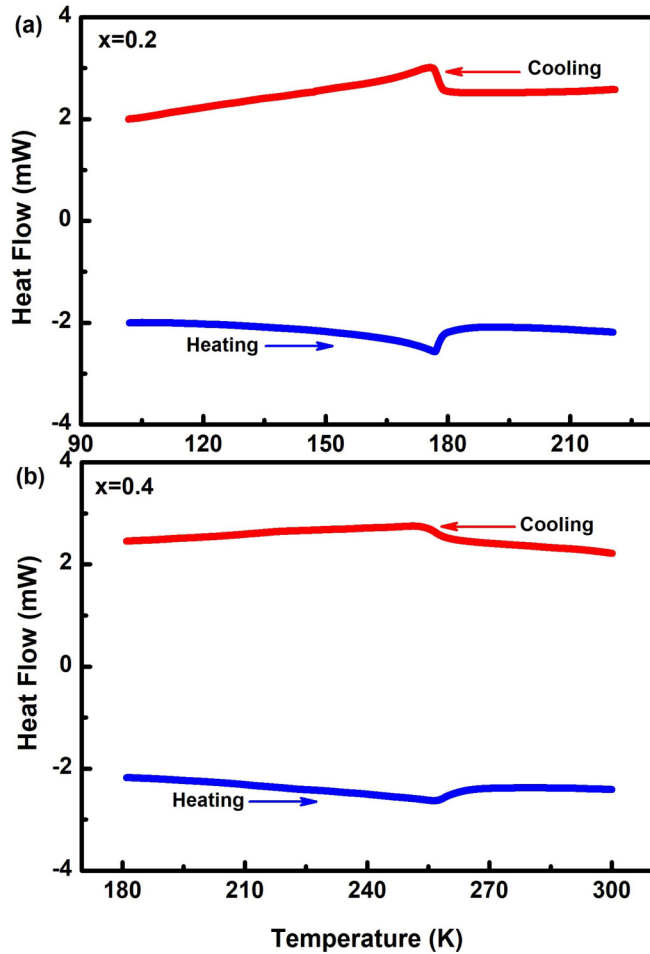
FIG. 4. DSC curves during cooling and heating processes at the scanning rate of 5 K/min for (a) $x = 0.2$ and (b) $x = 0.4$.

FIG. 5. Field-dependent magnetization isotherms for $NdCo_{2-x}Fe_x$ ($x = 0$, 0.2, 0.4, 0.6) compounds at various temperatures around T_C during field-decreasing (O) and -increasing (−) processes under applying magnetic field change of 0-6 T.

cubic structure to a FM tetragonal structure. The structural transition occurs at the same temperature as that of the magnetic transition temperature, indicating strong magnetoelastic coupling. In general, the structural transitions have been considered to be coupled with the FOMT, as evidenced in a number of typical systems such as YFe_4Ge_2 [44], $CaFe_2As_2$ [45], $Fe_{1+y}Se_xTe_{1-x}$ [46], and $CoFe_2O_4$ [47]. To confirm the nature of structural phase transitions in our samples, the DSC measurements in the heating and cooling cycles were performed for $x = 0.2$ and 0.4 samples as shown in Fig. 4. Both the samples show endothermic and exothermic peaks at their phase transition temperatures (177 K for $x = 0.2$, and 255 K for $x = 0.4$). Thermal curves show the long tail on the lower temperature side and no temperature difference between the exothermic and endothermic peaks is observed. Such hysteretic features belong to SOMT. These results clearly indicate that the structural transition is coupled to SOMT. On substituting Fe, the second-order nature of the transition remains unchanged, however, the transition spreads over a wide temperature range. Magnetostructural transitions with second order are known to be caused by the softening of the phonon mode and such a transition has also been observed in other compounds, e.g., $DyFe_4Ge_2$ [48], $TbCo_{2-x}Fe_2$ [30], $KMnF_3$ [49], and $La_{1.6}Nd_{0.35}CuO_4$ [50].

C. Field-dependent magnetization $M(H)$ and magnetocaloric effect

To analyze the MCE, the field-dependent magnetization $M(H)$ isotherms of $NdCo_{2-x}Fe_x$ ($x = 0$, 0.2, 0.4, and 0.6) were recorded at selected temperatures below and above T_C for a temperature interval of 3 K as shown in Fig. 5. As is known, the hysteresis loss is an important factor for refrigerant materials. To check the hysteresis loss and its effect on the MCE, the $M(H)$ curves were measured under field-decreasing (6-0 T) and field-increasing (0-6 T) processes. The open circles denote a representative field-decreasing process, while the solid lines correspond to the field-increasing process. The magnetization decreases with increasing temperature for all the compositions; signifying the magnetic transition from a low-temperature FM to a high-temperature PM phase. It is interesting to note that in the FM state ($T < T_C$), a large proportion of the change in magnetization occurs at low field ($H < 1.5$ T). This feature is favorable for magnetic refrigeration applications at low fields. The $M(H)$ curves coincide well with each other during cooling and heating processes around T_C and thus there exists a negligible hysteresis even at low fields at all measured temperatures. This perfect reversibility of magnetic transition is desirable for practical applications in magnetic refrigeration. Obviously, it is attributed to the second-order nature of a magnetic transition from PM to FM.

By using measured $M(H)$ curves, the ΔS_M around the FM-PM phase transition temperature was derived according to the Maxwell equation as follows: [14,63]

$$\Delta S_M = \int_0^H \left(\frac{\partial M}{\partial T} \right)_H dH, \tag{1}$$

where T is the absolute temperature and H is the applied magnetic field. For magnetization measured at the discrete
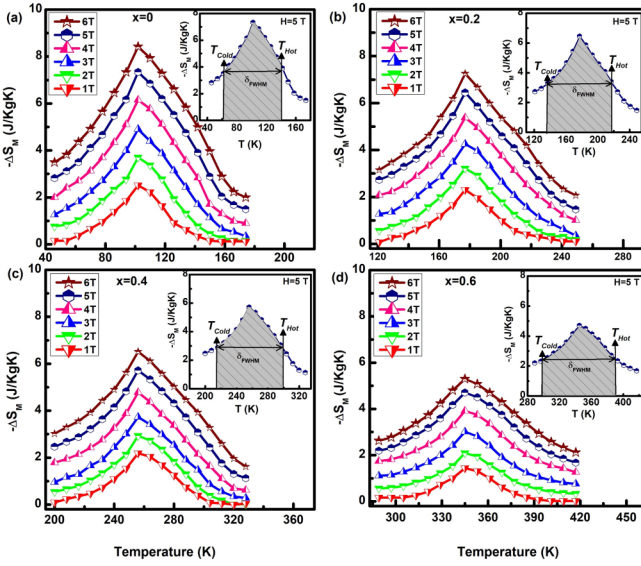
FIG. 6. Magnetic entropy change (ΔS_M) as a function of temperature (T) at different magnetic fields for the NdCo$_{2-x}$Fe$_x$ (a) $x = 0$ (b) $x = 0.2$ (c) $x = 0.4$, (d) $x = 0.6$. The insets show the $\Delta S_M - T$ curve for $H = 5$ T. The shaded area corresponds to the RCP.

field and temperature intervals, the ΔS_M can be described as

$$\Delta S_M = \sum_i \frac{M_{i+1} - M_i}{T_{i+1} - T_i} \Delta H_i, \qquad (2)$$

where M_{i+1} and M_i represent the magnetization measured at temperatures T_{i+1} and T_i respectively, under H_i field. The calculated ΔS_M values at various applied magnetic fields are shown in Fig. 6. For each composition, the maximum ΔS_M occur near the T_C, and ΔS_M increases linearly with the increasing field, which together with the symmetrical broadening of the ΔS_M peak are the features of the SOMT. The position of the peak shows a negligible shift as the field changes from 1 T to 6 T. The maximum values of ΔS_M for NdCo$_2$, NdCo$_{1.8}$Fe$_{0.2}$, NdCo$_{1.6}$Fe$_{0.4}$, and NdCo$_{1.4}$Fe$_{0.6}$, are found to 3.7 Jkg^{-1}K^{-1}, 3.21 Jkg^{-1}K^{-1}, 2.93 Jkg^{-1}K^{-1}, and 2.09 Jkg^{-1}K^{-1} for a field change of 2 T and 7.33 Jkg^{-1}K^{-1}, 6.45 Jkg^{-1}K^{-1}, 5.71 Jkg^{-1}K^{-1}, and 4.70 Jkg^{-1}K^{-1} for a field change of 5 T. Although substitution of Fe in the place of Co causes a decrease in the ΔS_M value, which is attributed to the decrease of the magnetic moment, the ΔS_M-T peak is found to be extended over a broad operating temperature (OT) range which is necessary for a good refrigerant material and can be defined as a difference between T_{Hot} and T_{Cold} (δT_{FWHM}) of ΔS_M-T around T_C [30]. For the $x = 0$ sample, the OT is 78 K at a field change of 5 T, while for the $x = 0.6$ sample, the OT range is 92 K. It indicates that the Fe substitution for Co in NdCo$_2$ has positive impact, i.e., it tunes the T_C from 102 K toward RT and increases the OT range for the MCE as well. It points out that the OT range of this system can be further increased by alloying with different Fe concentrations. Magnetic hysteresis effect, another important factor for magnetic refrigerant materials, was ignored in these calculations, since $M(H)$curves shows negligible hysteresis.

As we know, the RCP is an important parameter to evaluate the magnetocaloric performance of magnetic materials [64],

which is a measure of heat transfer between the cold and hot reservoirs in one ideal refrigerant cycle. The RCP can be estimated by integration of the ΔS_M-T curve over the FWHM as follows:

$$\text{RCP} = \int_{T_{\text{Cold}}}^{T_{\text{Hot}}} |\Delta S| dT, \qquad (3)$$

where integration limits (T_{Cold} and T_{Hot}) are the temperatures corresponding to the half-maximum values at the two sides of the ΔS_M peak. The calculated RCP values for NdCo$_2$, NdCo$_{1.8}$Fe$_{0.2}$, NdCo$_{1.6}$Fe$_{0.4}$, NdCo$_{1.4}$Fe$_{0.6}$ are 153.8 Jkg^{-1}, 149.7 Jkg^{-1}, 142.8 Jkg^{-1}, 98.8 Jkg^{-1} for a field change of 2 T and 529.96 Jkg^{-1}, 497.25 Jkg^{-1}, 470.55 Jkg^{-1}, 428.31 Jkg^{-1} for a field change of 5 T. For NdCo$_2$, the ΔS_M spans over a wide temperature range of 48 T and 78 K under field change of 2 T and 5 T, respectively, and corresponding RCP values are 153.8 Jkg^{-1} and 529.96 Jkg^{-1}. These results imply that the NdCo$_2$ is also a potential refrigerant material working at low temperature. As a comparison, the magnetocaloric properties including ΔS_M, OT range, and RCP for NdCo$_{2-x}$Fe$_x$ (present paper), and other R-based reported materials [42,63–65] for the magnetic field changes of 2 T and 5 T are summarized in Table II. As seen in Table II, although NdCo$_{2-x}$Fe$_x$ possesses a moderate ΔS_M values, however, the OT range is much broader than that for previously reported Gd and some of R-based giant MCE materials under the same magnetic field change. Such a wide OT range yields large RCP values and is important for practical applications. These merits may make NdCo$_{2-x}$Fe$_x$ compounds promising refrigerant materials for magnetic refrigerants over a wide temperature range, including room temperature. These results were obtained from polycrystalline samples, (which have an averaging effect from different grains); however, for single crystal or oriented samples of the NdCo$_{2-x}$Fe$_x$ system, we expect excellent magnetocaloric performance.

IV. CONCLUDING REMARKS

In conclusion, a systematic and detailed investigation of the MCE of NdCo$_{2-x}$Fe$_x$ ($0 \leqslant x \leqslant 0.6$) compounds has been carried out. The temperature dependent synchrotron x-ray diffraction analysis reveals that the samples $x = 0$ and 0.4, undergo a structural phase transition from a cubic to tetragonal phase with decreasing temperature, which is coupled with the magnetic phase transition. Importantly, all the samples exhibit the SOMT. DSC results have shown the absence of thermal hysteresis in the magnetic transition region. The partial replacement of Co for Fe in NdCo$_2$ not only increases the magnetic transition temperature but also broadens the MCE OT range from 78 K for NdCo$_2$ to 92 K for NdCo$_{1.4}$Fe$_{0.6}$, leading to the increasing of RCP. These MCE parameters, i.e., OT and RCP, are comparable to Gd, Gd$_5$Ge$_2$Si$_2$ and even larger than and some recently reported R-based potential magnetic refrigerant materials at field changes of 2 T and 5 T. These merits may make NdCo$_{2-x}$Fe$_x$ compounds a suitable and attractive candidate for magnetic refrigeration. The present paper not only helps in understanding the MCE near the PM-FM phase transition in R-based materials but it also demonstrates the feasibility of developing novel magnetocaloric materials with a wide working temperature range and large RCP values.

TABLE II. Comparison of the magnetic entropy change (ΔS_M), operating temperature range (OT), and relative cooling power (RCP) values of $NdCo_{2-x}Fe_x$ compounds with other magnetic materials for a magnetic field change of 2 T and 5 T.

			2 T			5 T		
Compound	T_C (K)	$-\Delta S_M$ ($Jkg^{-1}K^{-1}$)	OT range (K)	RCP Jkg^{-1}	$-\Delta S_M$ ($Jkg^{-1}K^{-1}$)	OT range (K)	RCP Jkg^{-1}	Ref.
$Dy_{12}Co_7$	64	4.9	30	102	10	42	425	[51]
DyFeSi	70	9.2	15	80	17.4	18	225	[52]
Dy_3Al_2	94	7.3	25	153	12.1	67	472	[53]
$ErCo_{1.8}Mn_{0.2}$	97	2.8	49	124	6.97	67	467	[54]
$NdCo_2$	102	3.7	48	153.8	7.33	78	529.96	Present paper
$Er_{0.5}Gd_{2.5}Co$	110	4.1	43	165	11	63.2	518	[55]
Gd_3Co	129	4.5	43	169	11.1	60	505.4	[56]
$Gd_8Tb_4Co_7$	140	3.5	32	120	8.2	51	316	[56]
$DyCo_2$	143	10.03	20	175	12.85	35	345	[57]
Gd_2Ir_2Sn	154	3.9	45	176	7.3	58	423	[58]
$Gd_{12}Co_7$	163	4.6	38	171	8.8	71.7	462.8	[56]
$NdCo_{1.8}Fe_{0.2}$	177	3.21	51	149.7	6.45	82	497.25	Present paper
$Pr_{0.775}Sr_{0.225}MnO_3$	175	1.9	45	90	3.59	81	292.54	[59]
$DyCo_{1.92}Fe_{0.08}$	175	2.5	49	95	5.22	69	293	[57]
$CeFe_{1.98}Al_{0.02}$	178	0.6	43	25.8	1.5	68	103	[60]
$DyCo_{1.8}Mn_{0.2}$	222	2.6	43	102.6	4.57	59.08	270	[54]
$Tb_{0.8}Dy_{0.2}Co_2$	224	3.5	35	120	5.76	62	369	[61]
$CeFe_2$	228	1.8	37	72	3.8	52	141	[60]
$TbCo_2$	234	3.61	26	115	6.9	50	357	[30]
$NdCo_{1.6}Fe_{0.4}$	255	2.93	53	142.8	5.71	85	470.55	Present paper
$HoCo_{1.76}Fe_{0.24}$	256	1.28	52	60	5.22	69	293	[57]
$TbCo_{1.94}Fe_{0.04}$	275	1.9	49	92	3.9	89	299	[30]
$Gd_5Ge_2Si_2$	276	6.5	16	104	18.6	25	442.7	[33]
Gd	294	5	49	214	9.5	70	410	[32]
$MnFeP_{0.45}As_{0.55}$	305	14.5	15	224	18	39	414	[62]
$TbCo_{1.8}Mn_{0.2}$	315	1.62	35	62.5	3.20	63.12	202	[54]
$NdCo_{1.4}Fe_{0.6}$	345	2.09	55	98.8	4.70	92	428.31	Present paper

[1] S. B. Roy and P. Chaddah, Curr. Sci. **88**, 71 (2005).

[2] Z. W. Ouyang, F. W. Wang, Q. Hang, W. Liu, G. Liu, J. Lynn, J. Liang, and G. Rao, J. Alloys Compd. **390**, 21 (2005).

[3] V. K. Pecharsky and K. Gschneidner, Adv. Mater. **13**, 683 (2001).

[4] E. Gratz and A. Markosyan, J. Phys.: Condens. Matter **13**, R385 (2001).

[5] R. Z. Levitin and A. S. Markosyan, Usp. Fiz. Nauk **155**, 623 (1988).

[6] R. Z. Levitin and A. S. Markosyan, Sov. Phys. Usp. **31**, 730 (1988).

[7] R. Z. Levitin and A. S. Markosyan, J. Magn. Magn. Mater. **84**, 247 (1990).

[8] A. M. Tishin and Y. Spichkin, *The Magnetocaloric Effect and Its Application* (Institute of Physics Publishing, Bristol, 2003).

[9] K. A. Gschneidner, V. Pecharsky, and A. Tsokol, Rep. Prog. Phys. **68**, 1479 (2005).

[10] B. Sattibabu, A. Bhatnagar, K. Vinod, and A. Mani, Physica B **514**, 37 (2017).

[11] A. Boutahar, R. Moubah, H. Lemziouka, A. Hajjaji, H. Lassri, and E. K. Hlil, J. Magn. Magn. Mater. **444**, 106 (2017).

[12] M. Balli, D. Fruchart, and D. Gignoux, J. Alloys Compd. **509**, 3907 (2011).

[13] N. A. de Oliveira, J. Alloys Compd. **403**, 45 (2005).

[14] K. A. Gschneidner and V. K. Pecharsky, Annu. Rev. Mater. Sci. **30**, 387 (2000).

[15] F. X. Hu, J. Wang, L. Chen, J. L. Zhao, J. R. Sun, and B. G. Shen, Appl. Phys. Lett. **95**, 112503 (2009).

[16] H. Wada, S. Matsuo, and A. Mitsuda, Phys. Rev. B **79**, 092407 (2009).

[17] R. C. Floresand, V. Franco, A. Conde, K. E. Knipling, and M. A. Willard, Appl. Phys. Lett. **98**, 102505 (2011).

[18] S. Paticopoulos, R. C. Flores, V. Franco, J. Blazquez, A. Conde, and K. E. Knipling, Solid State Commun. **152**, 1590 (2012).

[19] V. Franco, K. R. Pirota, V. M. Prida, Antonio Maia J. C. Neto, A. Conde, M. Knobel, B. Hernando, and M. Vazquez, Phys. Rev. B **77**, 104434 (2008).

[20] A. Nirmala, A. Morozkin, and S. Malik, Pramana-J. Phys. **84**, 977 (2015).

[21] J. Cwik, J. Solid State Chem. **209**, 13 (2014).

[22] J. Cwik, K. Nenkov, I. Tereshina, and T. Palewski, Mater. Chem. Phys. **136**, 492 (2012).

[23] C. M. Bonilla, J. Herrero-Albillos, F. Bartolome, L. M. Garcia, M. Parra-Borderias, and V. Franco, Phys. Rev. B **81**, 224424 (2010).

[24] M. E. Wood and W. H. Potter, Cryogenics **25**, 667 (1985).

[25] N. K. Singh, K. G. Suresh, A. K. Nigam, S. K. Malik, A. A. Coelho, and S. Gama, J. Magn. Magn. Mater. **317**, 68 (2007).

[26] A. Rowe, Int. J. Refrig. **34**, 168 (2011).

[27] Z. W. Ouyang, F. W. Wang, Q. Huang, W. F. Liu, Y. Q. Xiao, J. W. Lynn, J. K. Liang, and G. H. Rao, Phys. Rev. B **71**, 064405 (2005).

[28] Y. G. Xiao, Q. Huang, Z. W. Ouyang, J. W. Lynn, J. K. Liang, and G. H. Rao, J. Alloys Compd. **420**, 29 (2006).

[29] M. S. Anikin, E. N. Tarasov, N. V. Kudrevatykh, and A. V. Zinin, Solid State Phenom. **233**, 247 (2015).

[30] M. Halder, S. M. Yusuf, M. D. Mukadam, and K. Shashikala, Phys. Rev. B **81**, 174402 (2010).

[31] W. G. Zheng, Y. Cui, F. Chen, Y. Shi, and D. Shi, J. Magn. Magn. Mater. **460**, 137 (2018).

[32] V. K. Pecharsky and K. A. Gschneidner, Phys. Rev. Lett. **78**, 4494 (1997).

[33] J. Shen, J. Wu, and J. Sun, J. Appl. Phys. **106**, 083902 (2009).

[34] J. Rodriguez-Corvajal, Physica B **192**, 55 (1993).

[35] See Supplemental Material at http://link.aps.org/supplemental/10.1103/PhysRevB.101.214427 for Fig. 1, which shows the synchrotron x-ray diffraction data with Rietveld refinement for NdCo$_{1.8}$Fe$_{0.2}$ (a) at 300 K (b) at 150 K and (c) for NdCo$_{1.4}$Fe$_{0.6}$ at 250 K.

[36] R. T. Macaluso and B. K. Greve, Dalton Trans. **41**, 14225 (2012).

[37] K. H. J. Buschow, Rep. Prog. Phys. **40**, 1179 (1977).

[38] J. C. Slater, J. Chem. Phys. **41**, 3199 (1964).

[39] A. Kowalczyk, A. Szajek, J. Baszynski, J. Kovac, and G. Chelkowska, J. Magn. Magn. Mater. **166**, 237 (1997).

[40] A. Kowalczyk, J. Baszynski, J. Kovac, and A. Szlaferek, J. Magn. Magn. Mater. **176**, 241 (1997).

[41] M. Foldeaki, A. Giguere, R. Chahine, and T. Bose, Adv. Cryog. Eng. **43**, 1533 (1998).

[42] A. S. Arrott, Phys. Rev. B **31**, 2851 (1985).

[43] S. Yang and X. Ren, Phys. Rev. B **77**, 014407 (2008).

[44] P. Schobinger-Papamantellos, J. Rodríguez-Carvajal, G. André, N. Duong, K. H. J. Buschow, and P. Toledano, J. Magn. Magn. Mater. **236**, 14 (2001).

[45] N. Ni, S. Nandi, A. Kreyssig, A. I. Goldman, E. D. Mun, S. L. Bud'ko, and P. C. Canfield, Phys. Rev. B **78**, 014523 (2008).

[46] S. Li, C. de la Cruz, Q. Huang, Y. Chen, J. W. Lynn, J. Hu, Y.-L. Huang, F.-C. Hsu, K.-W. Yeh, M. K. Wu, and P. Dai, Phys. Rev. B **79**, 054503 (2009).

[47] S. Yang, X. Ren, and X. Song, Phys. Rev. B **78**, 174427 (2008).

[48] P. Schobinger-Papamantellos, J. Rodríguez-Carvajal, G. André, and K. H. J. Buschow, J. Magn. Magn. Mater. **300**, 333 (2006).

[49] G. S. ad J. Minkiewicz and A. Lisz, Solid State Commun. **8**, 1941 (1970).

[50] B. Keimer, R. J. Birgeneau, A. Cassanho, Y. Endoh, M. Greven, M. A. Kastner, and G. Shirane, Z. Phys. B **91**, 373 (1993).

[51] Q. Dong, J. Chen, X. Zhang, X. Zheng, J. Sun, and B. Shen, J. Appl. Phys. **114**, 173911 (2013).

[52] H. Zhang, Y. Sun, E. Niu, L. Yang, and J. Shen, Appl. Phys. Lett. **103**, 202412 (2013).

[53] Y. W. Li, H. Zhang, T. Yan, K. W. Long, H. S. Wang, Y. J. Xue, C. Cheng, and H. B. Zhou, J. Alloys Compd. **651**, 278 (2015).

[54] A. K. Pathak, I. Dubenko, S. Stadler, and N. Ali, J. Magn. Magn. Mater. **323**, 2436 (2011).

[55] Z. J. Mo, J. Shen, L. Q. Yan, J. F. Wu, C. C. Tang, and B. G. Shen, J. Appl. Phys. **113**, 033908 (2013).

[56] Z. G. Zheng, X. C. Zhong, H. Y. Yu, Z. W. Liu, and D. C. Zeng, J. Appl. Phys. **109**, 07A919 (2011).

[57] M. Anikina, E. Tarasov, N. Kudrevatykh, A. Inishev, M. Semkin, A. Volegov, and A. Zinin, J. Magn. Magn. Mater. **418**, 181 (2016).

[58] K. Schafer, C. Schwickert, O. Niehaus, F. Winter, and R. Pöttgen, Solid State Sci. **35**, 66 (2014).

[59] S. Banik and I. Das, J. Magn. Magn. Mater. **460**, 234 (2018).

[60] A. Haldar, K. G. Suresh, and A. K. Nigam, J. Phys. D: Appl. Phys. **43**, 285004 (2010).

[61] Y. Zeng, F. Tian, T. Chang, K. Chen, S. Yang, K. Cao, C. Zhou, and X.Song, J. Phys.: Condens. Matter **29**, 055804 (2017).

[62] O. Tegus, E. Bruck, K. Buschow, and F. de Boer, Nature (London) **415**, 150 (2002).

[63] T. Hashimoto, T. Numasawa, M. Shino, and T. Okada, Cryogenics **21**, 647 (1981).

[64] M. D. Mukadam and S. M. Yusuf, Physica B **405**, 686 (2010).

[65] U. Atzmony, M. Dariel, and G. Dublon, Phys. Rev. B **14**, 3713 (1976).